

An Investigation of Characteristics of the Operating Modes of Two-Module Thyristor Controlled Series Compensator

Gyo-Bum Chung

Dept. of Electrical Engineering, Hongik University
Jochiwon, Chungnam, 339-701, Korea

Phone: +82-415-60-2595, Fax: +82-415-60-2376, E-mail: gbchung@wow.hongik.ac.kr

Abstract - This paper aims at investigating the characteristics of the operating modes of two-module Thyristor Controlled Series Compensator (TCSC) in a power transmission system. The operating modes of two-module TCSC are defined, analyzed and compared to those of single-module TCSC. The load flow program, the stability calculation program and Electro Magnetic Transient Program (EMTP) simulation of a TCSC power transmission system are developed for the performance evaluation of two-module TCSC as a power flow controller. In the process of the simulation study, the potential problem areas of the TCSC power transmission system are identified.

1. Introduction

Thyristor-Controlled Series Compensator (TCSC) can improve the power transfer capability of a power transmission system, damp the real power oscillation and compensate the impedance of the transmission line from capacitive range to inductive range [1]. A TCSC module consists of a series capacitor and parallel paths with a thyristor switch and a surge inductor, a metal-oxide varistor for overvoltage protection and a bypass breaker. The operating modes of a single module TCSC in a power transmission system are

classified into the full conduction mode (FM), the Vernier mode (VM), and the Blocked mode (BM) [1]. The BM TCSC has no gate signals of thyristors and zero thyristor conduction. The FM TCSC has continuous gate signal of thyristors. The VM TCSC has phase control of gate signals of thyristors and consequent partial thyristor conduction. A complete TCSC power transmission system may be comprised of several such modules in series to improve power system performance [1,2]. The operating modes of the multi-module TCSC are the combination of FM, VM, and BM. Using two-module TCSC power transmission system shown in Fig. 1, the approximate equivalent of operating modes of the multi-module TCSC in a power transmission system can be obtained.

In order to investigate the characteristics of the operating modes in a two-module TCSC power transmission system, the load flow calculation, the stability analysis and EMTP simulations are performed for the combinations of BM and VM and of FM and VM with emphasis on power flow control. Comparison between the characteristics of operating modes of a single module TCSC and those of operating modes of a two-module TCSC are also made. In the process of the simulation study, the potential problem areas of TCSC circuit are identified.

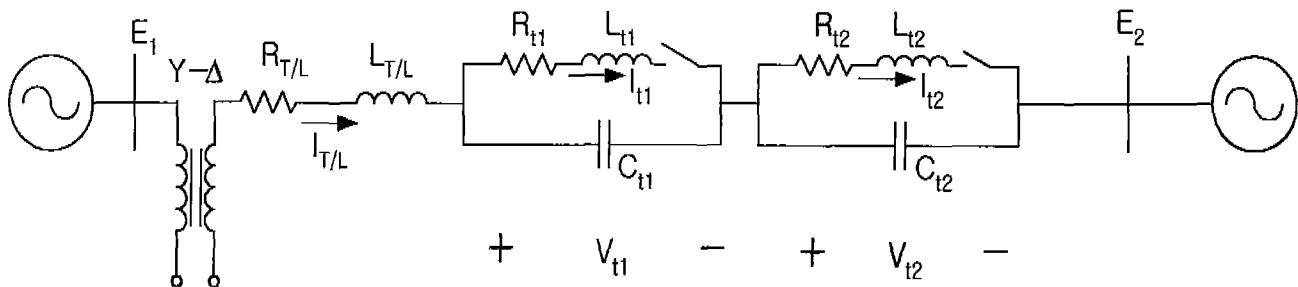


Fig. 1 The single-phase diagram of a simple power transmission system with two-module TCSC

2. Load Flow Calculation

Fig. 2 shows the relation between the thyristor conduction angle of TCSC module and the compensated power flow supplied by the system voltage E_1 in Fig. 1. The power flow controlled by TCSC depends on the thyristor conduction angle of TCSC modules, which is determined by the gate-firing instant and the power system parameters.

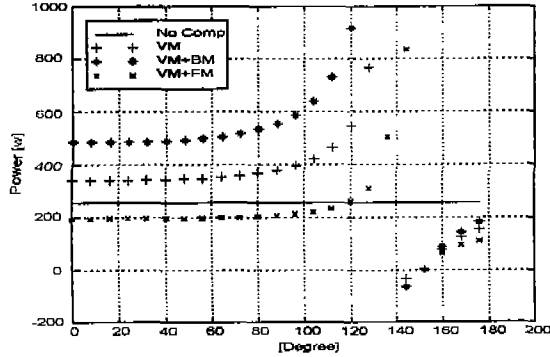


Fig. 2 The real power flows compensated by a single-module TCSC system and by a two-module TCSC for various operating modes versus the conduction angle.

The conduction angle and the power flows in the TCSC power transmission system are determined by the gate-firing instants of the thyristors. In order to obtain the information of the gate-firing instants of thyristors, the power flows, the voltages in the TCSC power transmission system, which are essential for the evaluation of the performance of the TCSC power system, the load flow calculation are performed.

For the load flow calculation, the switching function, $H_1(\omega t)$, describing the operation of thyristors of the TCSC module 1, is used, which has a value of one when a thyristor is on and zero when the thyristor is off [3,4,5]. The complex Fourier series representation of the switching function, $H_1(\omega t)$, is

$$H_1(\omega t) = \sum h_n(\sigma_1, \psi_1) e^{jn\omega t} \quad (1)$$

where h_n is a function of the thyristor conduction angle, σ_1 , and the gate firing instant ψ_1 [3]. The capacitor voltage of TCSC module 1, $V_{c1}(\omega t)$, expressed in the complex Fourier series is

$$V_{c1}(\omega t) = \sum V_{cn} e^{jn\omega t} \quad (2)$$

The inductance current of TCSC module 1, $I_{l1}(\omega t)$, expressed in complex Fourier series is

$$I_{l1}(\omega t) = Y_{l1} H_1(\omega t) V_{c1}(\omega t) \quad (3)$$

where Y_{l1} is the admittance matrix of the TCSC inductance branch. With the Thevenin's equivalent impedance matrix of the power transmission system except TCSC modules, Z_{TH} , and the admittance matrix of the TCSC capacitance branch, Y_c , the terminal voltage of TCSC module 1, V_{t1} , are written as

$$V_{t1} = (Y_{l1} \cdot H_1 + Y_{c1})^{-1} \cdot I_{TL} \quad (4)$$

where the transmission line current I_{TL} , is

$$I_{TL} = \frac{E_1 - E_2}{[Z_{TH} + (Y_{l1}H_1 + Y_{c1})^{-1} + (Y_{l2}H_2 + Y_{c2})^{-1}]^{-1}} \quad (5)$$

Then the real power flow, P_1 , supplied by the system voltage E_1 in Fig. 1, are written as

$$P_1 = 3 \cdot E_1^*(\omega t) \cdot I_{TL}(\omega t) = g(\sigma_1, \psi_1, \sigma_2, \psi_2) \quad (6)$$

where E_1^* is the conjugate of E_1 . If the values of σ and ψ in Eq. (6) were known, the real power, P_1 , the harmonic voltage vector V_t and the current vector I_t could be easily found.

For the control scheme of the TCSC power transmission system, an equidistant firing and constant σ controller is used [3]. To find the values of σ_1 , ψ_1 for the first module and σ_2 , ψ_2 for the second module, two additional equations are used from the conditions that the thyristor currents are zero at the turn-off instants.

$$I_{l1}(\psi_1 + \sigma_1) = 0, \quad I_{l2}(\psi_2 + \sigma_2) = 0 \quad (7)$$

With the Bisection method in numerical methods, the thyristor gate-firing angles ψ_1 and ψ_2 can be found simultaneously for a given value of the real power flow, P_1 , of Eq. (6) [5].

3. Stability Analysis

The stability analysis of operating modes of two-module TCSC power transmission system is performed using the Poincare mapping from nonlinear dynamical systems theory [6]. The system state vector $X(t)$ of the combined operation of BM and VM are written as

$$X(t) = [I_{T1}(t), I_{I2}(t), V_{I2}(t), V_{E1}(t)]^T \quad (8)$$

During the conduction time of each of the thyristors, the system dynamics are described by the following set of linear differential equations:

$$\frac{dX(t)}{dt} = A \cdot X(t) + B \cdot E(t) \quad (9)$$

where A is the constant system matrix and B is the constant matrix, shown in Appendix 1.

During the off time of each thyristor, the system dynamics are expressed as

$$\frac{dX(t)}{dt} = P_{off} \cdot A \cdot X(t) + P_{off} \cdot B \cdot E(t) \quad (10)$$

where P_{off} is the projection matrix for off time of thyristors of TCSC module 1 [3,4,5].

From the Poincare mapping theory, the stability of the TCSC power transmission system depends on the eigenvalues of the Jacobian Df, which is defined as

$$Df(X_0, \psi_1) = (e^{P_{off} \cdot A \cdot (\frac{T}{2} - \sigma)} \cdot P_{off} \cdot e^{A \sigma})^2 \quad (11)$$

For the stable operation, the eigenvalues of Df lies inside the unit circle.

The stability analysis of the combined operation of FM and VM is similarly proceeded

Fig. 3 shows the magnitude of the eigenvalues versus the thyristor conduction angle of the single-module TCSC power transmission system. The single module operation is stable over the full range of the conduction angle. Fig. 4 shows the magnitude of the eigenvalues of the combined operation of VM and BM. Fig. 5 shows the magnitude of the eigenvalues of the combined operation of VM and FM. The magnitude of the eigenvalues of two-module operation is less than 1, which means the TCSC power transmission system stable.

4. EMTP Simulation Study

The investigation of the characteristics of the two-module TCSC in a power transmission system is performed by the computer simulation using EMTP. The EMTP simulation study includes the individual representation of the thyristors and other circuit components, as well as the various control functions

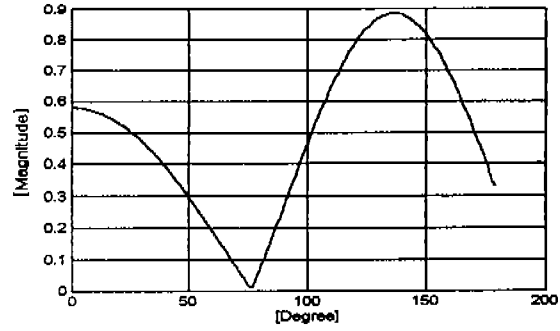


Fig. 3 The magnitude of the eigenvalues versus the thyristor conduction angle σ of the single module TCSC power transmission system.

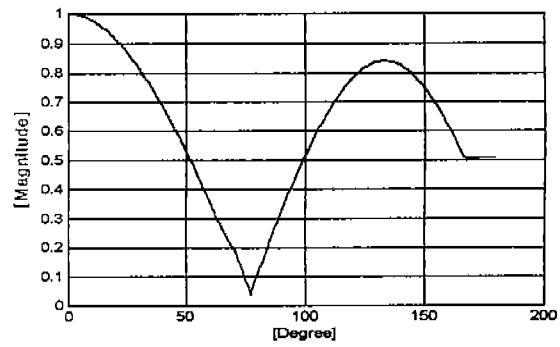


Fig. 4 The magnitude of the eigenvalues versus the thyristor conduction angle σ of the two- module TCSC (VM+BM) power transmission system.

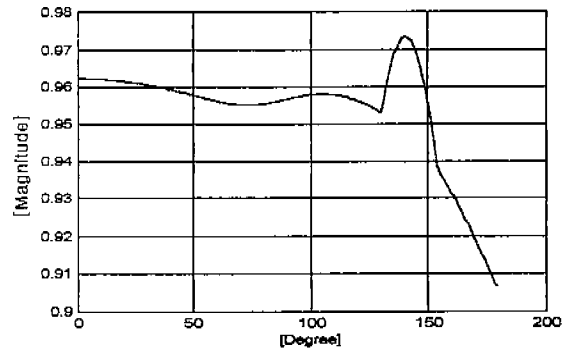


Fig. 5 The magnitude of the eigenvalues versus the thyristor conduction angle σ of the two- module TCSC (VM+FM) power transmission system.

and signal processing elements within TCSC module. Appendix 2 shows the parameters of the TCSC system shown in Fig. 1.

The system is initially operating without compensation, transmitting $P_o=257[W]$ and $Q_o=503[Var]$ at a phase angle difference 40° from E_1 to E_2 buses.

Fig. 6 shows the capacitor voltage and the reactor current of the single module TCSC system with the phase angle of gate-firing signal $\varphi=169.7^\circ$ obtained by the load flow calculation, the conduction angle $\sigma=80^\circ$, transmitting $P_{comp}=369.2[W]$ and $Q_{comp}=637[Var]$. Fig. 7 shows that the phase of the capacitor voltage of TCSC lags the T/L current by 90° , so the effective impedance of the TCSC module is capacitive. Fig. 8 and 9 shows the transient performance of the power flows caused by the insertion of a single module of TCSC. The waveforms show that the power flows

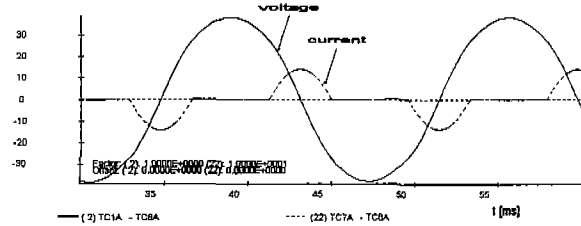


Fig. 6 The capacitor voltage and the reactor current of the single module TCSC power transmission system.

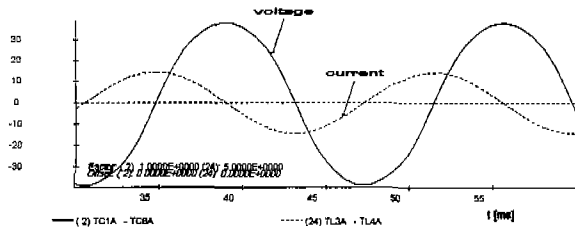


Fig. 7 The capacitor voltage and the T/L current of the single module TCSC power transmission system.

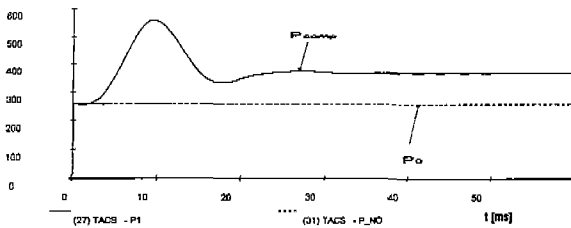


Fig. 8 The uncompensated real power flow P_o and the real power flow, P_{comp} , compensated by a single module TCSC.

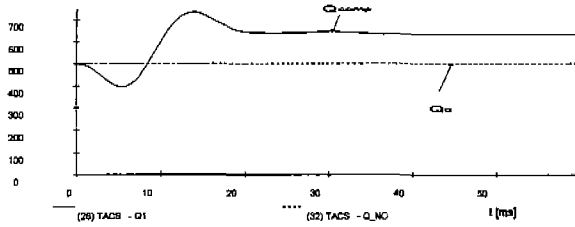


Fig. 9 The uncompensated reactive power flow Q_o and the reactive power flow, Q_{comp} , compensated by a single module TCSC.

change quickly and smoothly to its new power level, and the overshoot is well damped quickly, which is predicted by the eigenvalues. The steady state performance of TCSC power system in EMTF simulation using the phase angle of gate-firing signals obtained by the load flow calculation agrees with the load flow calculation.

The waveforms of Fig. 10 to Fig. 13 correspond with those of Fig. 6 to Fig. 9 except the conduction angle $\sigma=160^\circ$, transmitting $P_{comp}=90[W]$ and $Q_{comp}=228[Var]$, which means the effective impedance of the

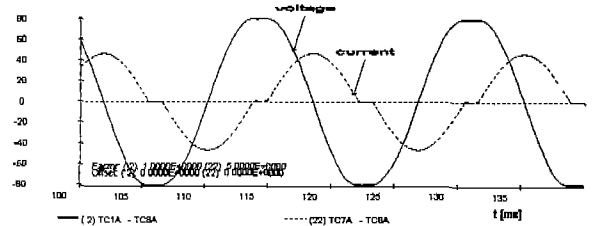


Fig. 10 The capacitor voltage and the reactor current of a single module TCSC power transmission system.

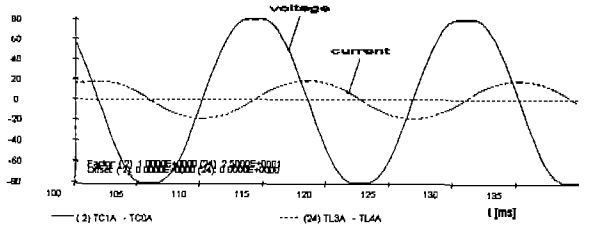


Fig. 11 The capacitor voltage and the T/L current of a single module TCSC power transmission system.

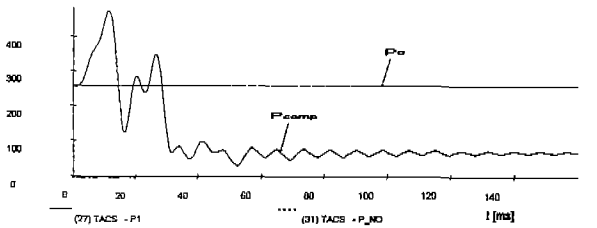


Fig. 12 The uncompensated real power flow and the real power flow compensated by a single module TCSC.

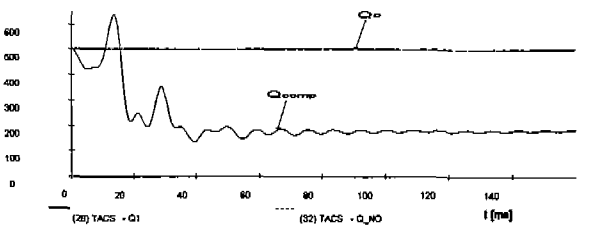


Fig. 13 The reactive power flows uncompensated and compensated by a single module TCSC.

TCSC module inductive. The transient response caused by the insertion of the inductive TCSC is also damped well, although somewhat oscillatory.

Fig. 14 and 15 show the waveforms of the single-module TCSC power transmission system, transmitting $P_{comp}=800[W]$ in the single-module TCSC power transmission system with $\sigma=125^\circ$ and $\varphi=130^\circ$ obtained by the load flow calculation.

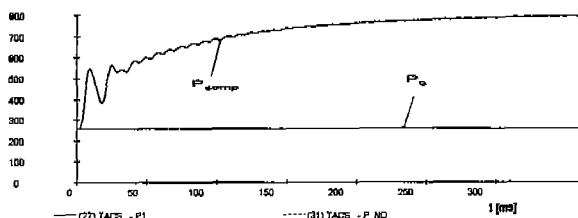


Fig. 14 The real power flow compensated by a single module TCSC with conduction angle $\sigma=125^\circ$.

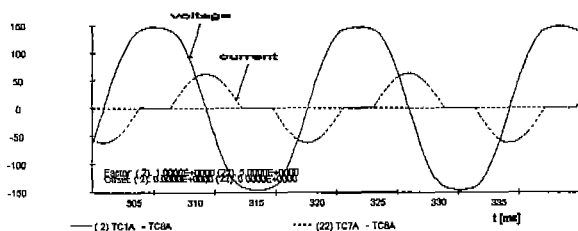


Fig. 15 The capacitor voltage and the reactor current of a single module TCSC with conduction angle $\sigma=125^\circ$.

Fig. 16 shows the transient response of real power, P_{comp} , after the insertion of the combination of the VM with $\sigma=80^\circ$ and the BM of two-module TCSC system. The combined operation of the two-module TCSC can transmit the real power more than that of the single-module TCSC after brief transient overshoots. Fig. 17 shows the capacitor voltage and the reactor current of the VM in the TCSC system.

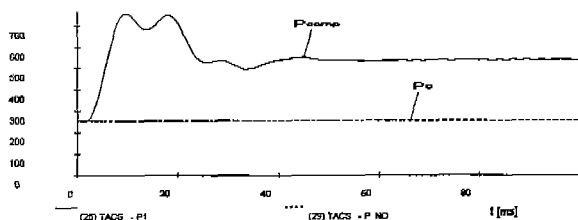


Fig. 16 The real power flow compensated by Vernier mode TCSC and Blocked mode TCSC in a power transmission system ($\sigma=80^\circ$).

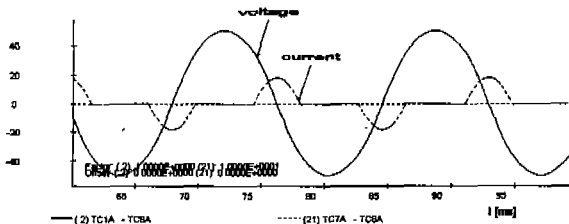


Fig. 17 The capacitor voltage of the reactor current of the Vernier mode TCSC in a two-module (VM+BM) TCSC power transmission system ($\sigma=80^\circ$).

Fig. 18 shows the transient response of power flow after the insertion of the combination of the VM with $\sigma=120^\circ$ and the BM of two-module TCSC system. P_{comp} is set to 800[W] which equals the real power flow in Fig. 14 to 15. Comparing with Fig. 14 and 15, the transient overshoot of the two-module operation is briefer than that of one-module operation, which means the multi-module is capable of faster response. Fig. 19 shows the capacitor voltage and the reactor current of the VM TCSC smaller than those of Fig. 15. It means that the required ratings of components of the multi-module TCSC operation are smaller than those of a single-module TCSC.

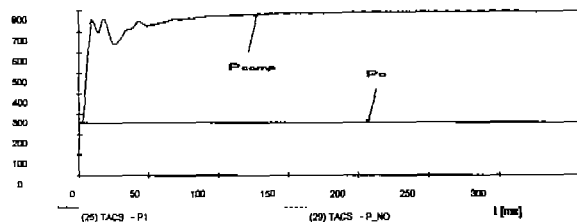


Fig. 18 The real power flow compensated by Vernier mode TCSC and Blocked mode TCSC in a power transmission system ($\sigma=120^\circ$).

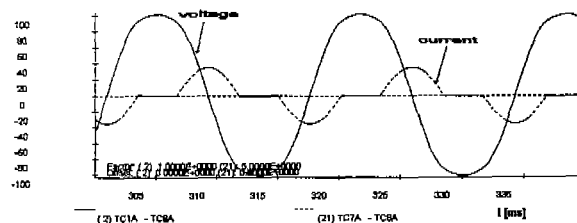


Fig. 19 The capacitor voltage and the reactor current of the Vernier mode TCSC in a two-module (VM+BM) TCSC power transmission system ($\sigma=120^\circ$).

Fig. 20 and Fig. 21 shows the waveform of the combined operation of the VM with $\sigma=164^\circ$ and the FM of two-module TCSC, transmitting $P_{comp}=90[W]$, which equals the real power flow in Fig. 10

to 13. The effective impedance of the two-module TCSC is inductive. Comparing with Fig. 10 to 13, the transient overshoot of the two-module operation lasts longer and more oscillatory, which is predicted by the magnitude of eigenvalues. Fig. 21 shows that the magnitude differences between the capacitor voltage and the reactor current of the VM TCSC and those of Fig. 10 are not very remarkable. It means that the TCSC modules operate more effectively in capacitive mode than in inductive mode.

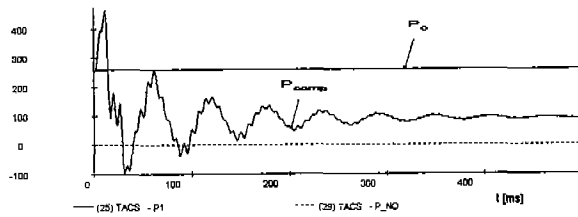


Fig. 20 The real power flow compensated by Vernier mode TCSC and Full conduction mode TCSC in a power transmission system ($\sigma = 164^\circ$).

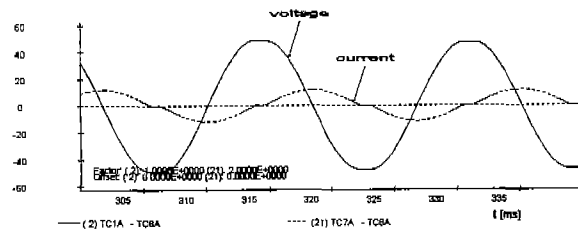


Fig. 21 The capacitor voltage and the reactor current of the Vernier mode TCSC with $\sigma = 164^\circ$ of a two-module TCSC (VM+FM).

5. Conclusion

In this paper, the load flow calculation, the stability analysis and the EMTF simulation of a TCSC power transmission system are performed to investigate characteristics of the operating modes of two-module TCSC as an equivalent of the multi-module TCSC.

Results of the load flow calculation using the complex Fourier series representation of the switching function agree with results of the EMTF simulation.

Comparing to the Vernier mode operation of single-module TCSC, two-module TCSC in the power transmission system increases the real power flow with faster and smooth transient response and requires smaller ratings of the TCSC components. However, the transient response of two-module TCSC to decrease the real power flow shows greater overshoot and longer settling time, predicted by the eigenvalues.

References

- [1] E.V. Larsen, et. al., "Characteristics and Rating Considerations of Thyristor Controlled Series Compensation," IEEE PES Paper 93-SM-433-3-PWRD, Vancouver, British Columbia, July 1993.
- [2] J. Urbanek, R.J. Piowko, E.V. Larsen, et al., "Thyristor Controlled Series Compensation Prototype Installation at the Slatt 500kV Substation," IEEE PES paper 92-SM-467-1 PWRD, Seattle, July 1992.
- [3] S.G. Jalali and R.H. Lasseter, "Harmonic Instabilities in Advanced Series Compensators," EPRI FACTS Conference, Boston, December, 1992, pp.1.4.3-1.4.28.
- [4] S.G. Jalali, I. Dobson and R.H. Lasseter, "Instabilities due to Bifurcation of Switching Times in a Thyristor Controlled Reactor," Proceedings of IEEE PESC'92, pp.546-552.
- [5] G.B. Chung et. al., "Analysis of the Operation of Thyristor Controlled Series Compensator interacting with Power System Components," in Proceeding of ITC_CSCC, pp. 741-744. Seoul, July 1996.
- [6] F. Verhulst, "Nonlinear Differential Equations and Dynamical Systems," Springer-Verlag, Berlin, 1990.

Appendix 1

The system matrix, A, and the constant matrix, B, and the projection matrix, $P_{T/L}$, are written as

$$A = \begin{bmatrix} -\frac{R_{T/L}}{L_{T/L}} & 0 & -\frac{1}{L_{T/L}} & -\frac{1}{L_{T/L}} \\ 0 & -\frac{R_{L2}}{L_{L2}} & \frac{1}{L_{L2}} & 0 \\ \frac{1}{C_{L2}} & -\frac{1}{C_{L2}} & 0 & 0 \\ \frac{1}{C_{L1}} & 0 & 0 & 0 \end{bmatrix} \quad (A-1)$$

$$B = \left[\frac{1}{L_{T/L}}, 0, 0, 0 \right]^T \quad (A-2)$$

$$P = \begin{bmatrix} 1 & 0 & 0 & 0 \\ 0 & 0 & 0 & 0 \\ 0 & 0 & 1 & 0 \\ 0 & 0 & 0 & 1 \end{bmatrix} \quad (A-3)$$

Appendix 2

The parameters of the TCSC power transmission system in Fig. 1 are ;

$$\begin{aligned} L_{L1} = L_{L2} = 20 \text{ mH}, \quad C_{L1} = C_{L2} = 244 \text{ }\mu\text{F} \\ R_{L1} = R_{L2} = 10^{-3} \text{ }\Omega, \quad L_{T/L} = 153 \text{ mH}, \quad R_{T/L} = 10 \text{ }\Omega \\ E_1 = 170 \cdot \cos(377 \cdot t + 30^\circ), \quad E_2 = 60 \cdot \cos(377 \cdot t - 10^\circ). \end{aligned}$$